Colloids and Surfaces B: Biointerfaces 185 (2020) 110619

Contents lists available at ScienceDirect

Colloids and Surfaces B: Biointerfaces

journal homepage: www.elsevier.com/locate/colsurfb

Dual function of interleukin-23 Aptamer to suppress brain inflammation via attachment to macrophage stimulating 1 kinase and interleukin-23

Hossein Shahdadi Sardou[a], Ali Jebali[b,c], Maryam Iman[a,*]

[a] Chemical Injuries Research Center, Systems Biology and Poisonings Institute, Baqiyatallah University of Medical Sciences, Tehran, Iran
[b] Molecular Medicine Research Center, Research Institute of Basic Medical Sciences, Rafsanjan University of Medical Sciences, Rafsanjan, Iran
[c] Medical Biotechnology Research Center, Ashkezar Branch, Islamic Azad University, Ashkezar, Yazd, Iran

ARTICLE INFO

Keywords:
Aptamer
Brain inflammation
Interleukin-23
MST1kinase

ABSTRACT

In the present study, the dual function of interleukin-23 (IL-23) Aptamer to suppress brain inflammation via attachment to macrophage stimulating 1 (MST1) kinase and IL-23, was introduced. Also, the anti-inflammatory property of IL-23 Aptamer has been investigated. This study showed that IL-23 Aptamer could reduce the clinical development of brain inflammation induced by Parathion, as an important organophosphate toxin. Both immunostaining and H&E staining indicated that the total inflammatory infiltration foci were remarkably decreased in IL-23 Aptamer-treated mice. Moreover, this study showed that IL-23 Aptamer reduced both absolute and relative numbers of MST1 + CD4 + Th1 cells and IL-23-producing cells. Analysis of the Hippo signaling genes showed a sharp decrease of *MST1* kinase compared with other genes ($P < 0.001$). Moreover, computer-assisted molecular docking demonstrated that both MST1 kinase and IL-23 could tightly attach to IL-23 Aptamer, and maybe block it. Taken together, IL-23 Aptamer coud decrease brain inflammation via suppressing MST1 kinase and IL-23.

1. Introduction

Different clinical reports support the correlation between the adaptive immune system and the Hippo signaling pathway [1–3]. Importantly, the Hippo signaling pathway links to various inflammatory mediators such as TNFα, IL-6, NF-κB, TLR, FoxO1/3, COX2, JAK/STAT, HIF-1α, and AP-1 [4]. A potential role of the Hippo signaling in the evolutionary expansion of the neocortex has been reported [5,6]. Generally, the Hippo signaling pathway regulates organ size in animals by regulating the cellular cycle and apoptosis [7]. The name of the pathway has been extracted from one of the main signaling proteins, the Hippo protein kinase [8]. The mutation in this gene makes overgrowth [9]. This pathway plays an imprtanat role in cell–cell contact, actin cytoskeleton, cell polarity, cellular energy, mechanical cues, and hormonal regulation [6,10]. The Hippo signaling network consists of co-activators, kinases, and DNA-binding partners [11]. The main co-activators are Yes-associated protein (YAP) and transcriptional co-activator with PDZ-binding motif (TAZ), and the main kinases are MST1 kinase and large tumor suppressor 1/2 (LATS1/2) [12]. When these proteins are activated, they translocate into the cellular nucleus to bind the transcriptional enhanced associate domain (TEAD) transcription factor [13]. This induces the expression of a wide range of genes. It has been shown that vestigial like family member 4 binds to TEAD and plays as a transcriptional repressor [14]. Importantly, the adaptor protein activates WW domain-containing protein 1, Ras-related proteins RAP2s (including three GTPases RAP2A/B/C), and MOB kinase activator [15]. On the other hand, the Hippo pathway interacts with bone morphogenetic proteins, Wingless/Ints, Notch, and Hedgehog. Moreover, these interactions regulate the activities of YAP and TAZ [16,17].

MST1 kinase, encoded by a specific gene, contains four domains and a serine protease which may not have any proteolytic activity. The receptor of MST1 kinase is RON tyrosine kinase, which stimulates epithelial lung cells. IL-23 is a heterodimeric cytokine. It has an IL12B (IL-12p40) and the IL23A (IL-23p19) subunit. IL-23 is a proinflammatory cytokine and is a key cytokine for Th17 maintenance and expansion [18].

Previously, our team found that the anti-inflammatory property of cerium oxide nanoparticles covered with interleukin-17 Aptamer [19]. In the present study, the anti-inflammatory property of IL-23 Aptamer was investigated. Also, the dual function of IL-23 Aptamer to suppress brain inflammation via blocking of two important molecules, MST1 kinase and interleukin-23, was introduced.

* Corresponding author.
E-mail address: iman1359@yahoo.com (M. Iman).

https://doi.org/10.1016/j.colsurfb.2019.110619
Received 7 August 2019; Received in revised form 25 October 2019; Accepted 28 October 2019
Available online 02 November 2019

2. Materials and methods

2.1. Materials

Nitrocellulose membrane, Parathion, hematoxylin and eosin (H&E) and Luxol Fast Blue (LFB) were provided from Sigma Company, Germany. All primers and Aptamer were purchased from TakapoZyzt Company, Iran. SYBR® Green Real-Time Master Mix, cDNA Mastermix, primary antibodies, and secondary antibody were purchased from Invitrogen, UK. RiboEx buffer was sourced from GeneAll company, South Korea.

2.2. Mice

Female Syrian mice, 4–8 weeks of age, were provided from Mashhad University of Medical Sciences, Mashhad. Iran. All experiments were in accordance with the guidelines of the National Institute of Health, and the ethics committee of Baqiyatallah University of Medical Sciences, Tehran. Iran (IR.BMSU.REC.1397.276). All mice were bred in pathogen-free cages, under constant temperature, and with free access to food.

2.3. Induction of brain inflammation and study groups

To prepare the brain inflammation model, we used Parathion toxin which before optimized [19]. The progression of model was scaled daily, where 0 = healthy, 1 = limp tail, 2 = hind limb weakness, 3 = paralysis of hind limb, 4 = tetraparalysis, and 5 = moribund/death. Then, mice were randomly divided into two groups: 1) treatment with IL-23 Aptamer intravenously with a dose of 100 pM from day 3 until day 10 (n = 5), and 2) control group which had brain inflammation, but had been treated with nothing (n = 5).

2.4. Histology and immunohistochemistry

After the treatment period, mice were euthanized, and their lumbar spinal cord was harvested. Then, they were fixed by Formaldehyde and embedded with paraffin. Consecutive 4 µm sections were taken, and slices were stained with H&E and LFB. For immunohistochemistry, sections were pre-incubated with the blocking buffer (1% BSA in PBS) for 2 h and then incubated with one of the following primary antibodies: anti-CD4, anti-IL-23, and anti-MST1. After 12 h at 4 °C, slices were washed and incubated with a secondary antibody. Finally, they were analyzed by fluorescent microscopy.

2.5. Flow cytometry analysis

After the treatment period, mice were euthanized, and their brain and spinal cord were collected in DMEM medium supplemented with 10% FBS, 100 U penicillin, 10 µg/mL streptomycin, 0.3 mg/mL L-glutamine, and 55 µM 2-mercaptoethanol. First, they were mechanically disrupted, and then enzymatically digested for 10 min at 37 °C. Then, they were filtered and washed with DMEM. Next, the cells were incubated with fluorochrome-labeled antibodies against CD4, IL-23 and MST1 at 4 °C for 20 min. Then, samples were acquired on a Flow cytometer. Instrument setup and calibration were performed daily using Cytometer Setup and Tracking beads.

2.6. Gene expression profile

To find the change of gene expression, five inflammatory genes were analyzed after treatment with IL-23 Aptamer. These genes were *IL-6, IL-23*, *IL-17, IL-10,* and *IFN-γ*. Moreover, we also investigated five Hippo signaling genes, including *YAP*, *TAZ*, *MST1*, *LATS1*, and *TEAD1* after the administration of IL-23 Aptamer. For the extraction of total RNA, RiboEx buffer was used. Then, 10 µL of cDNA Mastermix was added to 10 µL of total RNA and incubated at 50 °C for 60 min, to synthesize cDNA. Then, 2 µL of cDNA and 2 µL of forward/reverse primer were added to 4 µL of SYBR® Green Real-Time Master Mix and run by Real-time PCR machine (ABI 1 plus, USA). Finally, CT of each gene was recorded, and the relative expression of each gene was measured by ΔΔCT method. Here, *GAPDH* gene was as a house keeping gene.

2.7. Computer-assisted molecular docking

Docking was done by Ascalaph Designer software. Here, the known structure of IL-23 Aptamer with a surface domain of MST1 and IL-23p19 interacted for 50 ps. Based on the experimental data, the surface residues were defined as the interaction site, whereas no restraints were considered regarding Aptamer. The sequence of IL-23 Aptamer was 5́-(GGAGAA)-3́. As known, IL-23 is a heterodimeric cytokine and has two subunits, including IL12B (IL-12p40) and IL23A (IL-23p19).

2.8. Statistical analyses

In this study, all tests were done in triplicate, and data were presented as the mean ± SD. The unpaired two-tailed *t*-test and ANOVA were used for multiple groups followed by a *post hoc* analysis (Tukey with Levene's test $P > 0.05$). Here, *P*-values < 0.05 were considered statistically significant ($^{*}P < 0.05$, $^{**}P < 0.01$, $^{***}P < 0.001$).

3. Results

3.1. IL-23 Aptamer reduced the clinical development of brain inflammation

Based on Table 1, although peak score and disease onset were reduced in the treated group, disease incidence did not change in both groups. Analysis of clinical development in both groups showed a lower score of IL-23 Aptamer- treated mice from day 16 to day 28, compared with control. LFB staining (Fig. 1a) showed IL-23 Aptamer-treated mice had lower demyelination compared with mice which not treated with IL-23 Aptamer.

3.2. IL-23 Aptamer changed gene expression profile

Gene expression analysis (Fig. 1b) showed that the expression of *IL-10* was increased after treatment with IL-23 Aptamer. On the other hand, the expression of other inflammatory genes including *IL-23*, *IL-17, IL-6,* and *INF-gamma* was decreased. We also analyzed five Hippo signaling genes, including *YAP*, *TAZ*, *MST1*, *LATS1*, and *TEAD1* that their results were shown in Fig. 1c. The analysis showed that the expression of these genes was decreased after treatment with IL-23 Aptamer. Importantly, *MST1* had more affected than other genes ($P < 0.001$).

3.3. IL-23 Aptamer reduced inflammatory cells

Flow cytometry data (Fig. 2a) showed that the proportion of CD4 + T cells was reduced in the treated group. Also, both immunostaining (Fig. 2b) and H&E staining (Fig. 2c) demonstrated that the total inflammatory infiltration foci were remarkably decreased in IL-23 Aptamer-treated mice. On the other hand, this study showed that IL-23 Aptamer reduced both absolute and relative numbers of

Table 1
Clinical evaluation of mice with brain inflammation in control and treatment group.

group	Disease onset	Disease incidence	Peak score
Control (n = 5)	8.4	95%	3.5
IL-23 Aptamer (n = 5)	7	54%	1.2

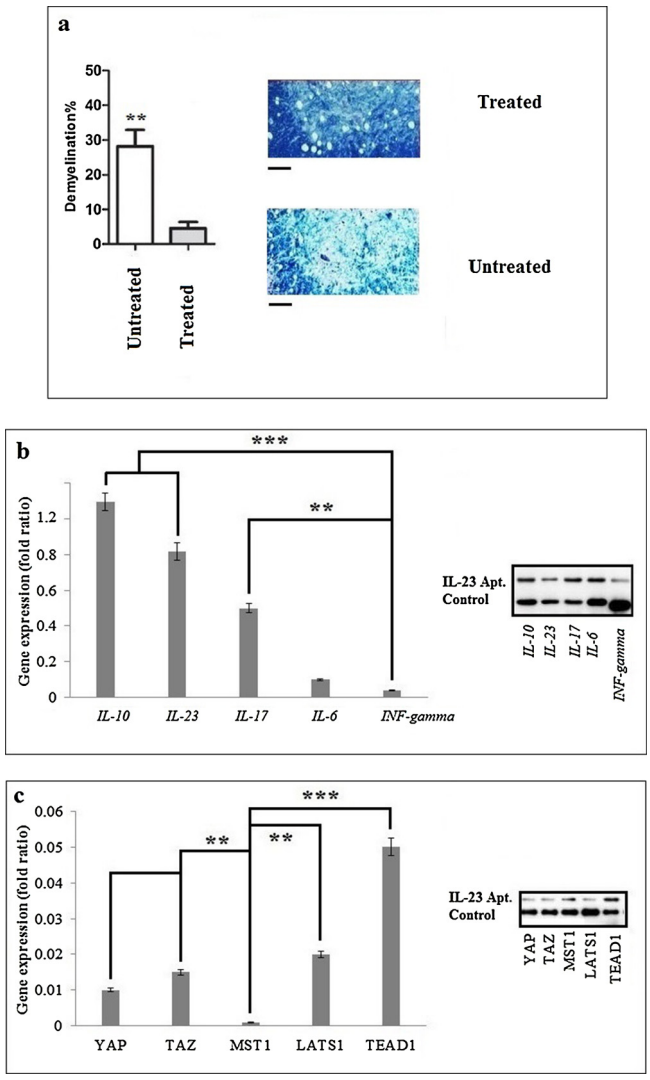

Fig. 1. Analysis of Luxol Fast Blue staining to find the quantity of demyelination (a) and clinical development (b) in both treated and untreated groups. Gene expression (b) of some important inflammatory genes. Gene expression (c) of the Hippo signaling pathway. N = 5, *P*-values < 0.05 were considered statistically significant (*$P < 0.05$, **$P < 0.01$, ***$P < 0.001$). Scale bar is 5 μm (For interpretation of the references to colour in this figure legend, the reader is referred to the web version of this article.).

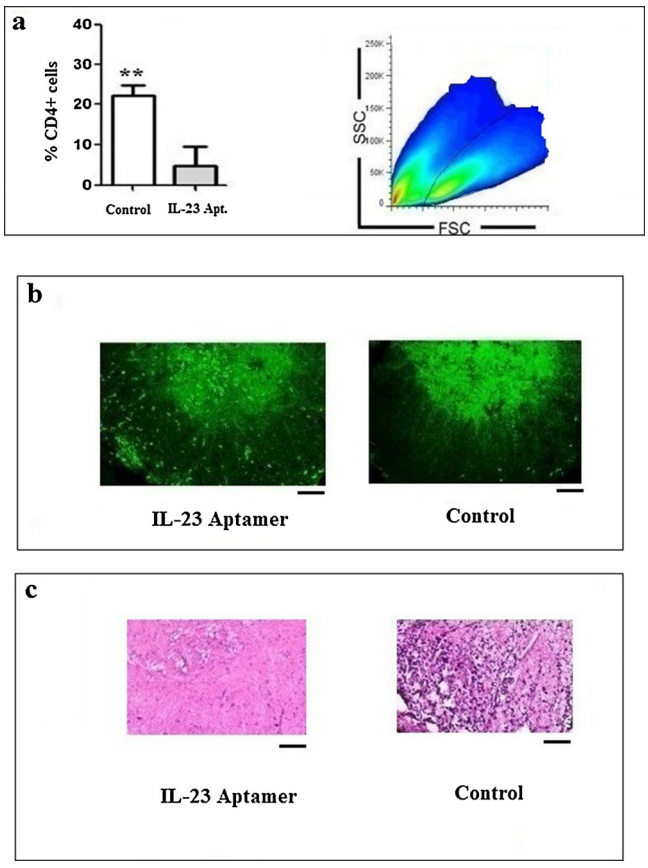

Fig. 2. Flow cytometry analysis (a), immunostaining (b), and H&E staining (c) of the spinal cord in control and treated groups. After the treatment period, mice were euthanized, and their lumbar spinal cord was harvested. Then, they were fixed by Formaldehyde and embedded with paraffin. Consecutive 4 μm sections were taken, and slices were stained with H&E and LFB. For immunohistochemistry, sections were pre-incubated with the blocking buffer (1% BSA in PBS) for 2 h and then incubated with one of the following primary antibodies: anti-CD4, anti-IL-23, and anti-MST1. After 12 h at 4 °C, slices were washed and incubated with a secondary antibody. N = 5, *P*-values < 0.05 were considered statistically significant (*$P < 0.05$, ***$P < 0.001$). Scale bar is 5 micrometer.

MST1 + CD4 + Th1 cells (Fig. 3 a–b) and IL-23-producing cells (Fig. 4 a–b).

3.4. Molecular docking

To find the interaction between IL-23 Aptamer and MST1 and between IL-23 Aptamer and IL-23, a computer-assisted molecular simulation was performed. Analysis of the 10 most favorable docking solutions showed that both MST1 and IL-23 can tightly attach to the Aptamer. The mean distance was below 10 Å for both groups. In agreement with the experimental data, the simulation analysis showed that MST1 as the main kinase of the Hippo pathway might be blocked by the Aptamer (Fig. 5a and b).

4. Discussion

In this study, it was shown that IL-23 Apatmer could reduce the clinical development of brain inflammation. Microscopic observations and flow cytometry analysis demonstrated that IL-23 Aptamer reduced the cellular infiltrates in the spinal cord, and the proportion of CD4 + T cells was sharply decreased in the treated group. Also, both immunostaining and H&E staining indicated that the total inflammatory infiltration foci were remarkably decreased in IL-23 Aptamer- treated mice. Moreover, IL-23 Aptamer decreased both absolute and relative numbers of MST1 + CD4 + Th1 cells and IL-23-producing cells. Gene expression analysis showed that the expression of *IL-10* was increased after treatment with IL-23 Aptamer. On the other hand, the expression of other inflammatory genes including *IL-23*, *IL-17, IL-6,* and *INF-gamma* was decreased. Analysis of the Hippo signaling genes showed a decrease of *MST1* kinase compared with other genes ($P < 0.001$). Analysis of the 10 most favorable docking solutions showed that both MST1 and IL-23 can tightly attach to the Aptamer. The docking analysis showed that MST1 as the main kinase of Hippo pathway might be blocked by the Aptamer.

Kinases and transcriptional molecules are in the center of the Hippo pathway. The most important kinases in this pathway are MST1/2, LATS1/2, mitogen-activated protein kinase, Salvador family WW domain-containing protein 1, MOB kinase activators, and Ras-related proteins [20]. Also, YAP, TAZ, and TEAD1–4 are the main transcriptional molecules. They activate the Hippo pathway by LATS1/2 kinases phosphorylate and inhibit YAP/TAZ [21]. It has been shown that phosphorylation of YAP/TAZ leads to proteasomal degradation and

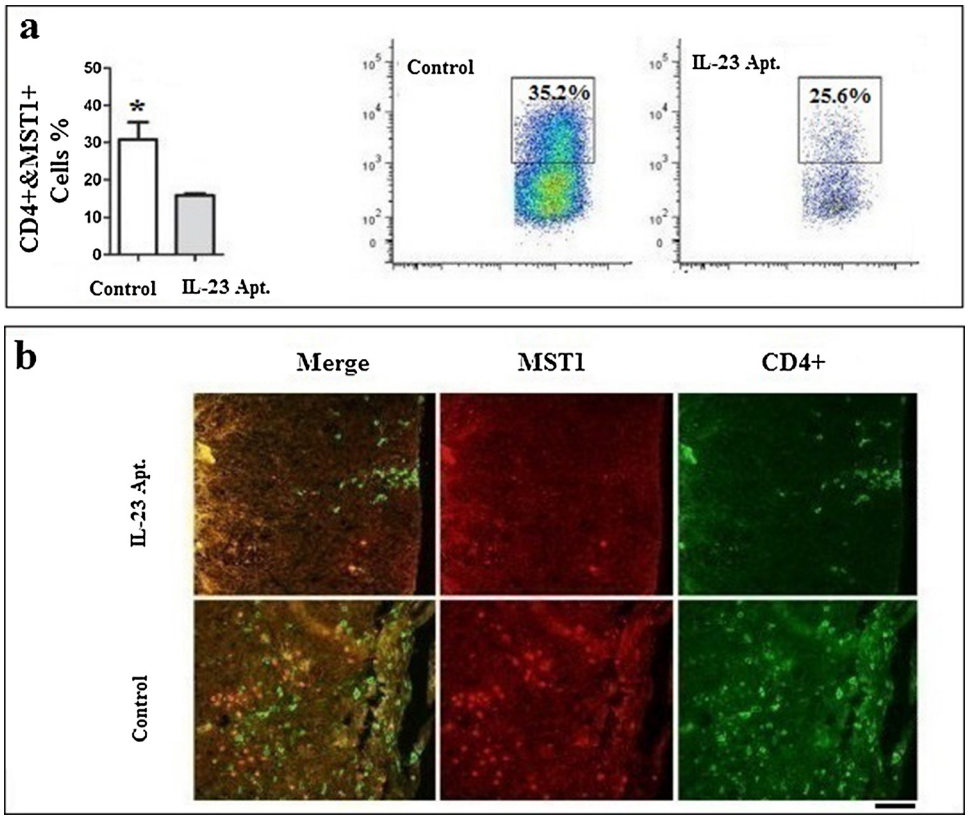

Fig. 3. The reduced number and percentage of MST1 + CD4 + Th1 cells obtained from flow cytometer (a) and immunostaining (b). After the treatment period, mice were euthanized, and their brain and spinal cord were collected in DMEM medium supplemented with 10% FBS, 100 U penicillin, 10 µg/mL streptomycin, 0.3 mg/mL L-glutamine, and 55 µM 2-mercaptoethanol. First, they were mechanically disrupted, and then enzymatically digested for 10 min at 37 °C. Then, they were filtered and washed with DMEM. Next, the cells were incubated with fluorochrome-labeled antibodies against MST1 at 4 °C for 20 min. N = 5, *P*-values < 0.05 were considered statistically significant (*P < 0.05, ***P < 0.001). Scale bar is 5 micrometer.

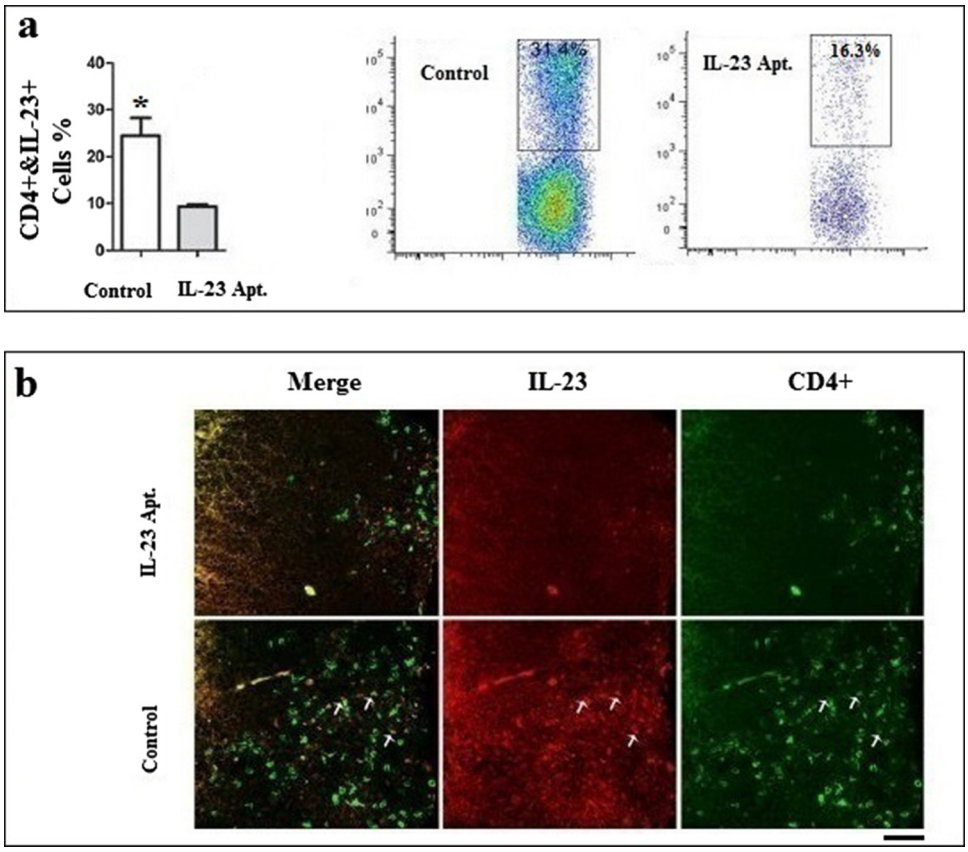

Fig. 4. The reduced number and percentage of IL-23-producing cells obtained from flow cytometer (a) and immunostaining (b). After the treatment period, mice were euthanized, and their brain and spinal cord were collected in DMEM medium supplemented with 10% FBS, 100 U penicillin, 10 µg/mL streptomycin, 0.3 mg/mL L-glutamine, and 55 µM 2-mercaptoethanol. First, they were mechanically disrupted, and then enzymatically digested for 10 min at 37 °C. Then, they were filtered and washed with DMEM. Next, the cells were incubated with fluorochrome-labeled antibodies against IL-23 at 4 °C for 20 min. N = 5, *P*-values < 0.05 were considered statistically significant (*P < 0.05, ***P < 0.001). Scale bar is 5 micrometer.

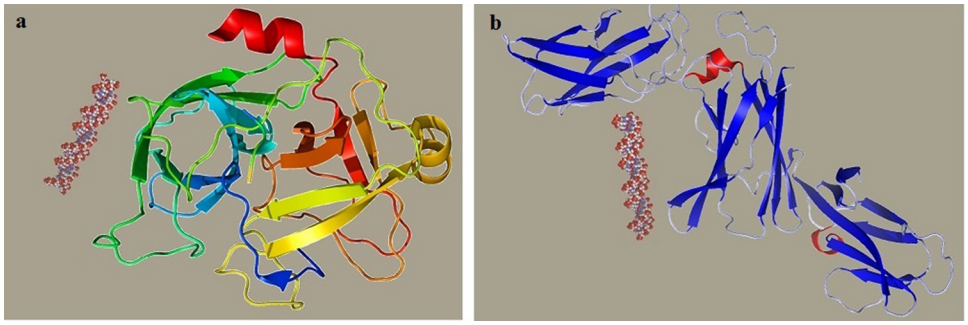

Fig. 5. Computer-assisted molecular docking between MST1 and IL-23 Aptamer (d) and between IL-23 and IL-23 Aptamer (e). Docking was done by Ascalaph Designer software. Here, the known structure of IL-23 Aptamer with a surface domain of MST1 and IL-23p19 interacted for 50 ps. The sequence of IL-23 Aptamer was 5́-(GGAGAA)-3́.

cytoplasmic retention [22]. In contrast, phosphorylated YAP/TAZ translocates into the nucleus to bind to TEAD1–4 and thus induces proliferation [23]. In addition to the physiological roles of the hippo signaling pathway, the recent studies have suggested intracellular mechanisms for this pathway. It is suggested that there is an important mechanism for inhibiting YAP by macrophages type II (M2), which prevents the clearance of inflamed cells. In addition, cell-mediated interference is controlled by YAP. The planned cell death and its ligand are the negative pathways, which prevents antigen detection by T cells. It has been widely accepted that the Hippo pathway acts as a tumor suppressor. It inhibits cell survival, proliferation, and tumorigenicity. Turning off the Hippo pathway is an inward cellular program to promote cell proliferation and survival, leading to cell proliferation and migration. The hyperactivity of YAP/TAZ is widespread in human neoplasms. Numerous reports suggest the gene amplification and epigenetic modulation of YAP /TAZ in cancer [24].

Poon et al showed that the Hippo Pathway regulates cellular diversity and brain size in *Drosophila melanogaster*. The inhibition of this pathway via depletion of Tao-1 leads to changes in neuroblasts during postembryonic neurogenesis [25]. Ramos et al showed the relationship between the Hippo signaling pathway and stem cell biology [16]. Plouffe et al demonstrated the main implications of the Hippo/YAP pathway. They stated that the increased cell proliferation and decreased apoptosis could be demonstrated by the dysregulation of the Hippo pathway [26]. Yu et al reported that the Hippo pathway could be regulated by G-protein-coupled receptor signaling. Also, serum-borne lysophosphatidic acid and sphingosine 1-phosphophate could inhibit the Hippo pathway [27]. Haskins et al found that ERBB4 activates YAP which is the main component of the Hippo pathway [28]. The receptor tyrosine kinase ERBB4 is a member of the epidermal growth factor receptor family.

5. Conclusion

Taken together, IL-23 Apatmer reduced the clinical development of brain inflammation in mice by reduction of the cellular infiltrates in the spinal cord. Also, both immunostaining and H&E staining indicated that the total inflammatory infiltration foci were remarkably decreased in IL-23 Aptamer-treated mice. Importantly, this study showed that IL-23 Aptamer could reduce MST1 + CD4 + Th1 cells and IL-23-producing cells. Gene expression analysis showed that the expression of *IL-10* was increased after treatment with IL-23 Aptamer. On the other hand, the expression of other inflammatory genes including *IL-23*, *IL-17, IL-6,* and *INF-gamma* was decreased. Analysis of the Hippo signaling genes showed a decrease of *MST1* kinase compared with other genes ($P < 0.001$). Analysis of docking interaction showed that both MST1 and IL-23 can tightly attach to IL-23 Aptamer.

Declaration of Competing Interest

There was no conflict of interest.

Acknowledgments

This article was financially supported by Baqiyatallah University of Medical Sciences, Tehran, Iran (grant ID: 91003251). All experiments were in accordance with the guidelines of the National Institute of Health, and ethics committee codes (IR.BMSU.REC.1397.276).

References

[1] L. Hong, X. Li, D. Zhou, J. Geng, L. Chen, Role of Hippo signaling in regulating immunity, Cell. Mol. Immunol. 15 (2018) 1003.
[2] T. Moroishi, T. Hayashi, W.-W. Pan, Y. Fujita, M.V. Holt, J. Qin, D.A. Carson, K.-L. Guan, The Hippo pathway kinases LATS1/2 suppress cancer immunity, Cell 167 (2016) 1525-1539. e1517.
[3] B. Liu, Y. Zheng, F. Yin, J. Yu, N. Silverman, D. Pan, Toll receptor-mediated Hippo signaling controls innate immunity in Drosophila, Cell 164 (2016) 406–419.
[4] Z. Taha, H. Janse van Rensburg, X. Yang, The Hippo pathway: immunity and cancer, Cancers 10 (2018) 94.
[5] Y. Wang, A. Yu, F.-X. Yu, The Hippo pathway in tissue homeostasis and regeneration, Protein Cell 8 (2017) 349–359.
[6] Z. Meng, T. Moroishi, K.-L. Guan, Mechanisms of Hippo pathway regulation, Genes Dev. 30 (2016) 1–17.
[7] J. Huang, S. Wu, J. Barrera, K. Matthews, D. Pan, The Hippo signaling pathway coordinately regulates cell proliferation and apoptosis by inactivating Yorkie, the Drosophila Homolog of YAP, Cell 122 (2005) 421–434.
[8] F.-X. Yu, Y. Zhang, H.W. Park, J.L. Jewell, Q. Chen, Y. Deng, D. Pan, S.S. Taylor, Z.-C. Lai, K.-L. Guan, Protein kinase A activates the Hippo pathway to modulate cell proliferation and differentiation, Genes Dev. 27 (2013) 1223–1232.
[9] K.F. Harvey, X. Zhang, D.M. Thomas, The Hippo pathway and human cancer, Nat. Rev. Cancer 13 (2013) 246.
[10] F.-X. Yu, B. Zhao, K.-L. Guan, Hippo pathway in organ size control, tissue homeostasis, and cancer, Cell 163 (2015) 811–828.
[11] B. Zhao, Q.-Y. Lei, K.-L. Guan, The Hippo–YAP pathway: new connections between regulation of organ size and cancer, Curr. Opin. Cell Biol. 20 (2008) 638–646.
[12] Y. Kwon, A. Vinayagam, X. Sun, N. Dephoure, S.P. Gygi, P. Hong, N. Perrimon, The Hippo signaling pathway interactome, Science 342 (2013) 737–740.
[13] L. Zhang, F. Ren, Q. Zhang, Y. Chen, B. Wang, J. Jiang, The TEAD/TEF family of transcription factor Scalloped mediates Hippo signaling in organ size control, Dev. Cell 14 (2008) 377–387.
[14] W. Zhang, Y. Gao, P. Li, Z. Shi, T. Guo, F. Li, X. Han, Y. Feng, C. Zheng, Z. Wang, VGLL4 functions as a new tumor suppressor in lung cancer by negatively regulating the YAP-TEAD transcriptional complex, Cell Res. 24 (2014) 331.
[15] T. Yamauchi, T. Moroishi, Hippo pathway in mammalian adaptive immune system, Cells 8 (2019) 398.
[16] A. Ramos, F.D. Camargo, The Hippo signaling pathway and stem cell biology, Trends Cell Biol. 22 (2012) 339–346.
[17] V. Fu, S.W. Plouffe, K.-L. Guan, The Hippo pathway in organ development, homeostasis, and regeneration, Curr. Opin. Cell Biol. 49 (2017) 99–107.
[18] C. Parham, M. Chirica, J. Timans, E. Vaisberg, M. Travis, J. Cheung, S. Pflanz, R. Zhang, K.P. Singh, F. Vega, A receptor for the heterodimeric cytokine IL-23 is composed of IL-12Rβ1 and a novel cytokine receptor subunit, IL-23R, J. Immunol. 168 (2002) 5699–5708.
[19] S. Hekmatimoghaddam, M. Iman, H.S. Sardo, A. Jebali, Gelatin hydrogel containing cerium oxide nanoparticles covered by interleukin-17 aptamar as an anti-inflammatory agent for brain inflammation, J. Neuroimmunol. 326 (2019) 79–83.
[20] A. Hergovich, Mammalian Hippo Signalling: A Kinase Network Regulated by Protein–Protein Interactions, Portland Press Limited, 2012.
[21] F.-X. Yu, J.-S. Mo, K.-L. Guan, Upstream regulators of the Hippo pathway, Cell Cycle 11 (2012) 4097.
[22] S. Piccolo, S. Dupont, M. Cordenonsi, The biology of YAP/TAZ: hippo signaling and beyond, Physiol. Rev. 94 (2014) 1287–1312.
[23] T. Moroishi, C.G. Hansen, K.-L. Guan, The emerging roles of YAP and TAZ in cancer, Nat. Rev. Cancer 15 (2015) 73.
[24] P. Friedl, S. Alexander, Cancer invasion and the microenvironment: plasticity and reciprocity, Cell 147 (2011) 992–1009.
[25] C.L. Poon, K.A. Mitchell, S. Kondo, L.Y. Cheng, K.F. Harvey, The Hippo pathway

regulates neuroblasts and brain size in Drosophila melanogaster, Curr. Biol. 26 (2016) 1034–1042.
[26] S.W. Plouffe, A.W. Hong, K.-L. Guan, Disease implications of the Hippo/YAP pathway, Trends Mol. Med. 21 (2015) 212–222.
[27] F.-X. Yu, B. Zhao, N. Panupinthu, J.L. Jewell, I. Lian, L.H. Wang, J. Zhao, H. Yuan, K. Tumaneng, H. Li, Regulation of the Hippo-YAP pathway by G-protein-coupled receptor signaling, Cell 150 (2012) 780–791.
[28] J.W. Haskins, D.X. Nguyen, D.F. Stern, Neuregulin 1–activated ERBB4 interacts with YAP to induce Hippo pathway target genes and promote cell migration, Sci. Signal. 7 (2014) ra116-ra116.